Fascinating Morphological Behavior of A₂-*star*-(B-*alt*-C) Molecules in the Melts and Solutions

Ching-I Huang, * *Yu-Lung Chang, Chih-Ming Chen*

Summary: We employ dissipative particle dynamics (DPD) to examine the self-assembling behavior of A₂-*star*-(B-*alt*-C) molecules in the melt and solution states. When these molecules are in the melts, we successfully observe various types of hierarchical structure-within-structures, such as A-formed spheres in the matrix formed by B and C alternating layers, hexagonally packed A-formed cylinders in the matrix with B and C segregated layers, B and C alternating layers-within-lamellae, coaxial B and C alternating domains within hexagonally packed BC-formed cylinders, and concentric BC-alternating domains within BC-formed spheres, by increasing the A composition. These hierarchical structures by varying the composition are reported theoretically for the first time in the copolymer systems consisting of the alternating blocks, and in good agreement with the most recent experimental work by Matsushita and co-workers (*Macromolecules* **2007**, *40*, 4023). Generally speaking, the small-length-scale B and C segregated domains are in parallel to the large-length-scale structures for the melt case. While when a selective solvent is added, we find that varying the solvent selectivity and the amount of solvent can induce the molecules to form quite different morphological patterns, such as the so-called segmented worm like micelles.

Keywords: coil-alternating molecule; dissipative particle dynamics; hierarchical structure; solvent selectivity

Introduction

With the improvement in synthetic techniques, copolymers with more complex forms of molecular architectures or with more than two types of monomers have been successfully formulated. These copolymers possess more diverse microstructures, which impose different influences upon various properties of polymers. Recently, copolymers with hierarchical structures have nowadays received high degrees of attention due to their potential applications as electrical, optical and other functional materials.[1–4]

Generally speaking, when the incompatibility degree between A and B is signifi-cant, traditional AB linear diblock copolymers form microphase-separated structures at only one characteristic length scale usually within 10–100 nm range. The morphology type is mainly dominated by the composition. When a third monomer type C is involved, copolymers often exhibit two-length-scale hierarchical structure-within-structure morphologies. Current research has mostly focused on the experimental studies of A-*block*-(B-*graft*-C) coil-comb copolymers.[2–12] There, the large-length-scale ordering morphology is mainly driven by the segregation between the A-coil blocks and the BC-comb blocks, and hence depends on the block composition. Once the interaction parameter between B and C becomes significantly large, a small-length-scale lamellar ordering of B and C segregation, which typically ranges between 1–10 nm, frequently occurs within

Institute of Polymer Science and Engineering, National Taiwan University, Taipei 10617, Taiwan
E-mail: chingih@ntu.edu.tw

WILEY InterScience®

the original BC-rich domains. In fact, coil-comb copolymers are not the only ones that can form hierarchical structures. By substituting the B-*graft*-C comb block with BC-alternating (denoted as B-*alt*-C) block, it is also possible to generate the small-length-scale structures within the large scale domains. Typical examples are copolymers containing a linear A-homopolymer block and a BC-alternating block with linear and simple graft (i.e., three-arm star) architectures, which are referred as A-*block*-(B-*alt*-C) and A$_2$-*star*-(B-*alt*-C), respectively. To our knowledge, there exist only a few relevant experimental studies by Matsushita group, which have addressed the formation of two-length-scale hierarchical structures on the multiblock copolymer with two or three chemically different monomers but different block lengths.[13–15] For example, they synthesized an undeca-block terpolymer consisting of two long poly(2-vinylpyridine) (P) end-blocks and short styrene (S)–isoprene (I) alternating middle-blocks, and observed the formation of spheres-within-lamellae, cylinders-within-lamellae, lamellae-within-lamellae, coaxial cylinders, and concentric spheres.[15] Though various types of unique hierarchical structures have been successfully obtained when three chemically different species are present in the copolymer systems containing the alternating blocks, the resulting phase behavior has not been fully understood from the theoretical point of view.

Herein, we employ the dissipative particle dynamics (DPD) simulation technique[16,17] to examine the self-assembling behavior of A$_2$-*star*-(B-*alt*-C) molecules in the melt and solution states. Generally speaking, the DPD method simplifies a long series of molecular groups into a few bead-and-spring type particles, and therefore it can simulate the molecular behavior on longer time-scales and larger length-scales compared with the classical molecular dynamics and Monte Carlo simulations. Our modeled chain, as displayed in Figure 1, consists of $2n$ alternating blocks of B and C, which is grafted into the middle
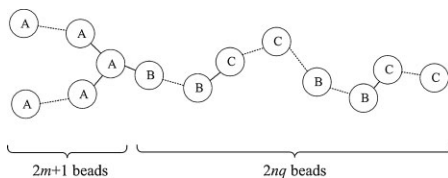
Figure 1.
Schematic plot of A$_2$-*star*-(B-*alt*-C) molecules.

of the coil A block with beads equal to $2m + 1$. Each B and C alternating block is represented by q beads. The total number of beads per chain N is thus equal to $(2m + 1) + 2nq$. We first set $q = 1$, i.e., each alternating block contains only one bead and indeed is very short. Accordingly, the stretching effects associated with the entropy and flexibility of chains can not be treated properly. To illustrate the effects of conformational freedom of each block, we increase q value to 2 and examine whether the resultant phase behavior is strongly influenced. In general, our simulated results for the melt case[18] have successfully captured most of the interesting morphology formation observed by experiments.

Computational Methods and Model Parameters

The DPD simulation method was originally proposed by Hoogerbrugge and Koelman.[16] The detailed formula can be found in refs. 17 and 19, and will not be reiterated here. In simulating the phase behavior by DPD, the particle mass m, the cut-off radius r_c, and the temperature k_BT are all set equal to 1, for convenience. The parameters γ and σ, which occur in the dissipative force and random force, respectively, are set to 4.5 and 3.0, respectively. The connecting pairs of beads in a molecule are assumed to interact via a linear spring with a harmonic spring constant C equal to 4. The DPD simulations are performed in a cubic box of L^3 grids with periodic boundary conditions. The particle density ρ is set equal to 3. Hence, the total simulated DPD beads

are $3L^3$. Initially these particles are started with a disordered configuration. Then the time evolution of the positions and velocities of all beads is carried out according to the velocity-Verlet algorithm with $\lambda = 0.65$ and the time step equal to 0.05. Each simulation is performed until the formed structure remains somewhat unchanged with the time step.

In the DPD simulations, the dimensionless interaction parameter (i.e., in terms of $k_B T$) between like particles $a_{II} = 25$ for the particle density $\rho = 3$ according to the work of Groot and Warren.[19] The interaction parameter between different components I and J can be estimated by the following relationship between a_{IJ} and the Flory-Huggins interaction parameter χ_{IJ} derived by Groot and Warren[19] for $\rho = 3$,

$$a_{IJ}(T) = a_{II} + 3.497\chi_{IJ}(T)$$

$$I, J = A, B, C, S$$

Therefore, the value of $a_{IJ} \leq 25$ corresponds to $\chi_{IJ} \leq 0$, which indicates that components I and J are very miscible. As the incompatibility between I and J increases, a_{IJ} increases from 25.

Results and Discussion

We first discuss the phase transition behavior associated with two-length-scale ordering for A_2-*star*-(B-*alt*-C) molecules, in which we use only one bead to represent each B and C block. Here we fix the value of $a_{AB} = a_{AC}$ at 100, which is significant enough to assure the formation of the large-length-scale diblock-like structures, and construct the corresponding phase diagram in terms of f_A and a_{BC} for $N = 13$, as shown in Figure 2. As can be seen clearly, a significant increase in the interaction parameter a_{BC} leads to the formation of small-length-scale B and C segregated lamellae within the large-length-scale BC-rich domains for the copolymers with values of f_A in a wide range of 0.2–0.85. In Figure 3 we display the various types of structure-within-structures, such as
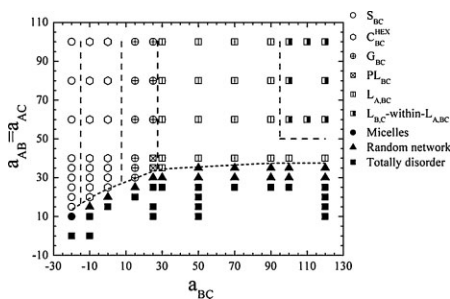
Figure 2.

Phase diagram of A_2-*star*-(B-*alt*-C) copolymers in terms of the interaction parameter $a_{AB} = a_{AC}$ and a_{BC} when $f_A = 0.54$, $q = 1$, and $N = 13$. The phase boundary lines are drawn to guide for the eyes.

A-formed spheres in the matrix formed by B and C alternating layers (S_A-within-$L_{B,C}$) ($f_A \cong 0.14$), hexagonally packed A-formed cylinders in the matrix with B and C segregated layers (C_A^{HEX}-
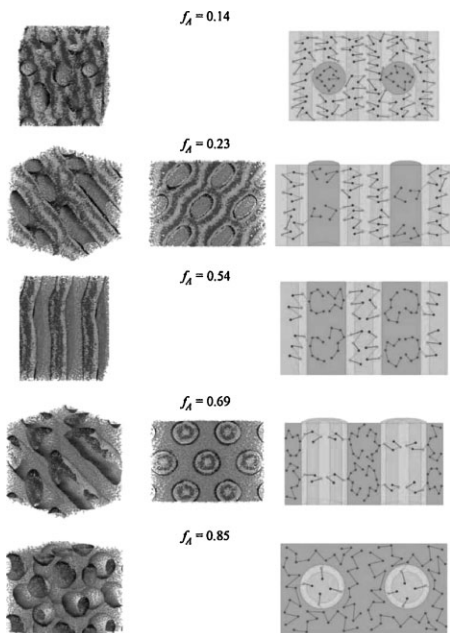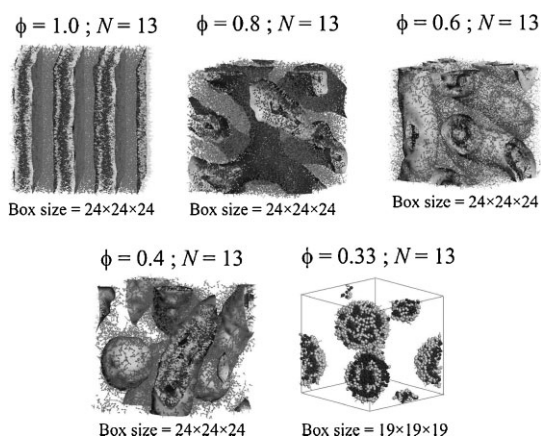

Figure 3.

Morphology variation and corresponding molecular arrangements of A_2-*star*-(B-*alt*-C) copolymers ($q = 1$, $N = 13$) with f_A when $a_{AB} = a_{AC} = 100$ and $a_{BC} = 120$. Note that the pattern when $f_A = 0.14$ corresponds to $N = 21$. The red, green, and blue colors represent A, B, and C, respectively. The red surface corresponds to the isosurface of component A.

within-$L_{B,C}$) ($f_A \cong 0.23$), $L_{B,C}$-within-$L_{A,BC}$ ($0.3 \leq f_A \leq 0.6$), coaxial B and C alternating domains within hexagonally packed BC-formed cylinders in the A-matrix ($L_{B,C}$-within-C_{BC}^{HEX}) ($0.65 \leq f_A \leq 0.7$), and concentric BC-alternating domains within BC-formed spheres in the A-matrix ($L_{B,C}$-within-S_{BC}) ($0.75 \leq f_A \leq 0.85$), which are simulated at $a_{BC} = 120$. Note that the two-length-scale morphology of S_A-within-$L_{B,C}$ shown in Figure 3 is obtained for the case of N increased to 21. This is simply because of the fact that in the original case of $N = 13$, the lowest value of f_A that the system can reach is 0.23. Accordingly, in order to observe whether the S_A-within-$L_{B,C}$ structure is possible to form at smaller values of f_A, we increase N to 21. Generally speaking, the geometry of large-length-scale morphology is mainly dominated by the composition f_A. This series of hierarchically ordered variation with the composition is in qualitatively good agreement with the most recent experimental work.[15] If we further examine the small-length-scale formation of B and C alternating layers within the major domains, such as C_A^{HEX}-within-$L_{B,C}$ and $L_{B,C}$-within-$L_{A,BC}$, it is clear that these layers are parallel to the A-formed cylinders or lamellae. This hierarchical periodicity along the same axis as

well as the various characteristic structures that the A_2-*star*-(B-*alt*-C) copolymers display are quite different from those in A-*block*-(B-*graft*-C) coil-comb copolymers. More interestingly, when f_A is larger than 0.5 so that B and C segregation occurs within the minor domains such as C_{BC}^{HEX} and S_{BC}, these BC-alternating chains fold in a particular way to form multiple (more than 2) B and C coaxial cylinders or concentric spheres. When we use more beads ($q = 2$) to represent each B and C alternating block, the resulting molecular packing behavior as well as the hierarchical structure types are quite similar. In more detail, the segregated B and C small-length-scale ordering is still observed in a parallel direction with respect to the diblock-like segregated large-length-scale structure. While, when a selective solvent is added, a completely different molecular packing behavior can be induced.

In order to manifest the influence of solvent addition, we choose an A-selective solvent S, in particular the interaction parameter $a_{AS} < a_{BS} = a_{CS}$. Figure 4 illustrates the morphology variation of A_2-*star*-(B-*alt*-C) copolymers ($q = 1$) with ϕ when $f_A = 0.54$, $N = 13$, $a_{AB} = a_{AC} = a_{BS} = a_{CS} = 100$, $a_{AS} = 25$, and $a_{BC} = 120$. It is clear that as ϕ decreases, these incompatible short B

$\phi = 1.0 ; N = 13$ $\phi = 0.8 ; N = 13$ $\phi = 0.6 ; N = 13$

Box size = 24×24×24   Box size = 24×24×24   Box size = 24×24×24

$\phi = 0.4 ; N = 13$ $\phi = 0.33 ; N = 13$

Box size = 24×24×24   Box size = 19×19×19

Figure 4.
Morphology variation of A_2-*star*-(B-*alt*-C) copolymers ($q = 1$) with ϕ when $f_A = 0.54$, $N = 13$, $a_{AB} = a_{AC} = a_{BS} = a_{CS} = 100$, $a_{AS} = 25$, and $a_{BC} = 120$.
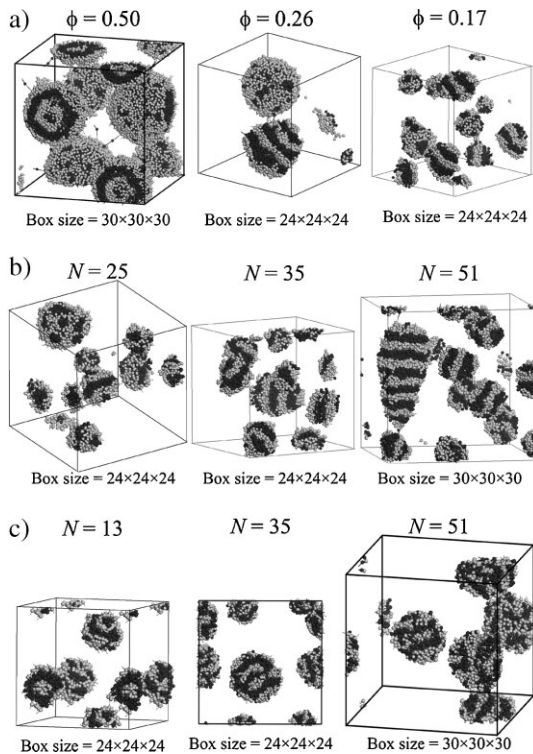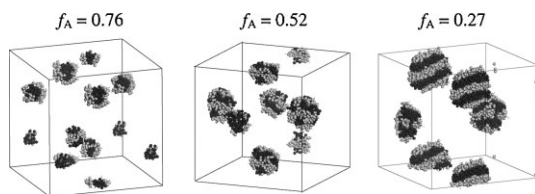
Figure 5.

Morphology variation of A_2-*star*-(B-*alt*-C) copolymer solutions with (a) ϕ when $q=2$, $f_A = 0.52$ and $N=33$, (b) N when $q=2$, $f_A = 0.52$ and $\phi = 0.2$, and (c) N when $q=1$, $f_A = 0.54$ and $\phi = 0.2$. All the interaction parameters are set as $a_{AB} = a_{AC} = a_{BS} = a_{CS} = 100$, $a_{AS} = 25$, and $a_{BC} = 120$.

and C blocks still form segregated lamellae within the BC-rich domains. The fact that adding a solvent S, which prefers the A block than the other B and C components, enables the large-length-scale structure to transform from lamellae → bicontinuous structure → BC-formed coaxial cylinders → BC-formed concentric spheres. This transition trend is analogous to decreasing the composition of B and C blocks in the melt. Indeed, it is not surprising since with an increase in the amount of solvent, the BC alternating blocks prefer to be near each other rather than the solvent and act like a minority component. If we take the conformational freedom of the short B and C blocks into account by using 2 beads to represent each B and C alternating block, we observe a similar transition of large-length-scale ordering as in the case of $q=1$. However, we find a very interesting phe-

nomenon when ϕ decreases to the formation of BC-formed spheres. For example, Figure 5(a) displays the morphological patterns of A_2-*star*-(B-*alt*-C) copolymers ($q=2$) with $f_A = 0.52$ and $N=33$ and the same interaction parameters as in Figure 4, $a_{AB} = a_{AC} = a_{BS} = a_{CS} = 100$, $a_{AS} = 25$, and $a_{BC} = 120$, when $\phi = 0.5$. As can be seen clearly, the B and C alternating blocks segregate to form concentric spheres at $\phi = 0.5$; but when ϕ decreases further, the B and C segregated domains tend to pack within the spherical (worm-like) micelles and form the so-called segmented worm-like micelles. By increasing the total number of beads per chain N, we also observe a similar transition within the BC-formed domains from a concentric to segmented packing (Figure 5(b)). Indeed, the so-called segmented worm-like micelles can be observed not only in the case of $q=2$

$f_A = 0.76$ $f_A = 0.52$ $f_A = 0.27$

Figure 6.
Morphological patterns of A$_2$-*star*-(B-*alt*-C) copolymers ($q = 2$) with $f_A = 0.76$, 0.52, and 0.27, respectively, when $N = 33$, $\phi = 0.11$, $a_{AB} = a_{AC} = a_{BS} = a_{CS} = 100$, $a_{AS} = 25$, and $a_{BC} = 120$.
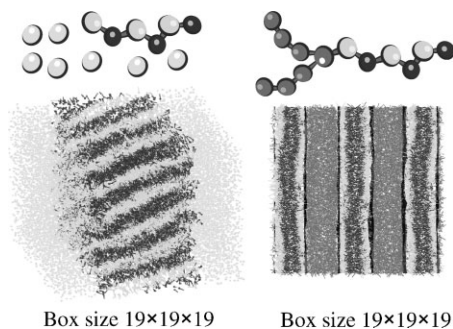
but also when $q = 1$, in which the total chain length N has to be larger (Figure 5(c)). Furthermore, we would like to address that when the formed micelles are inverted (BC alternating chain length longer than A), segmented worm-like micelles are more favored than co-centric spherical micelles. This can be seen very clearly in Figure 6, where we show the morphological patterns of A$_2$-*star*-(B-*alt*-C) copolymers ($q = 2$) with $f_A = 0.76$, 0.52, and 0.27, respectively, when $N = 33$, $\phi = 0.11$, $a_{AB} = a_{AC} = a_{BS} = a_{CS} = 100$, $a_{AS} = 25$, and $a_{BC} = 120$.

Finally, we would like to address why increasing the amount of solvent or the total chain length or the BC composition for the A$_2$-*star*-(B-*alt*-C) molecules in the presence of one A-selective solvent (in particular, $a_{AS} < a_{BS} = a_{CS}$) enables the formation of segmented worm-like micelles. Let us compare two limiting cases in Figure 7. One is the A$_2$-*star*-(B-*alt*-C) molecules in the melt, and the other one is the alternating B and C block molecules in the presence of solvent S, which is identical to A monomer but not connected with B-*alt*-C blocks. As the solvent S is neutral to both B and C, in order to have equal interfacial area with solvent S, the formed B and C segregated lamellae are packed in a perpendicular direction with respect to the BC- rich and S-rich domains. While in the melt, due to the fact that the A coil blocks are connected with a series of B and C alternating blocks, the formed B and C small-length-scale domains with respect to the large-length-scale lamellae, cylinders, and spheres, are typically parallel, coaxial, and concentric, respectively.

Box size 19×19×19   Box size 19×19×19

Figure 7.
Comparison of morphological patterns of B-*alt*-C molecules in one solvent S when $q = 1$, $N = 6$, and $\phi = 0.46$ and A$_2$-*star*-(B-*alt*-C) copolymer melt when $q = 1$, $N = 13$, and $f_A = 0.54$. The interaction parameters are set as $a_{AB} = a_{AC} = a_{BS} = a_{CS} = 100$ and $a_{BC} = 120$.

Summary

The self-assembling behavior associated with two-length-scale ordering of A$_2$-*star*-(B-*alt*-C) molecules in the melt and solution states is studied by dissipative particle dynamics (DPD). In particular, we assume that the interaction parameters between the coil A (solvent S) and the alternating B and C ($a_{AB} = a_{AC} = a_{SB} = a_{SC}$) are the same. When in the melt, various types of hierarchical structure-within-structures, such as A-formed spheres in the matrix of B and C alternating layers, A-formed cylinders in the matrix of B and C segregated layers, B and C alternating layers-within-lamellae, coaxial B and C alternating domains within cylinders, and

concentric BC-alternating domains within spheres, have been successfully observed. Generally speaking, the geometry of large-length-scale morphology is mainly dominated by the A composition. Due to the specific molecular architecture that the A coil blocks are connected with a series of B and C alternating blocks, the formed B and C small-length-scale domains are typically parallel with respect to the large-length-scale domains. When an A-selective solvent S is added, a series of large-length-scale ordering transition, which is analogous to decreasing the A composition in the melt, is expected. However, we find that by increasing the amount of solvent, the total chain length, and the BC composition, the B and C segregated domains can pack in a completely different way and form the so-called segmented worm-like micelles.

[1] M. Muthukumar, C. K. Ober, E. L. Thomas, *Science* **1997**, *277*, 1225–1232.

[2] J. Ruokolainen, R. Makinen, M. Torkkeli, T. Makela, R. Serimaa, G. ten Brinke, O. Ikkala, *Science* **1998**, *280*, 557–560.

[3] J. Ruokolainen, G. ten Brinke, O. Ikkala, *Adv. Mater.* **1999**, *11*, 777–780.

[4] R. Maki-Ontto, K. de Moel, W. de Odorico, J. Ruokolainen, M. Stamm, G. ten Brinke, O. Ikkala, *Adv. Mater.* **2001**, *13*, 117–121.

[5] J. Ruokolainen, M. Saariaho, O. Ikkala, G. ten Brinke, M. Torkkeli, R. Serimaa, *Macromolecules* **1999**, *32*, 1152–1158.

[6] O. Ikkala, G. ten Brinke, *Chem. Commun.* **2004**, 2131–2137.

[7] G. ten Brinke, O. Ikkala, *The Chemical Record* **2004**, *4*, 219–230.

[8] C. S. Tsao, H. L. Chen, *Macromolecules* **2004**, *37*, 8984–8991.

[9] E. Polushkin, S. Bondzic, J. de Wit, G. Alberda van Ekenstein, I. Dolbnya, W. Bras, O. Ikkala, G. ten Brinke, *Macromolecules* **2005**, *38*, 1804–1813.

[10] A. Laiho, R. H. A. Ras, S. Valkama, J. Ruokolainen, R. Osterbacka, O. Ikkala, *Macromolecules* **2006**, *39*, 7648–7653.

[11] W. van Zoelen, G. Alberda van Ekenstein, O. Ikkala, G. ten Brinke, *Macromolecules* **2006**, *39*, 6574–6579.

[12] S. Valkama, T. Ruotsalainen, A. Nykanen, A. Laiho, H. Kosonen, G. ten Brinke, O. Ikkala, J. Ruokolainen, *Macromolecules* **2006**, *39*, 9327–9336.

[13] Y. Nagata, J. Masuda, A. Noro, D. Cho, A. Takano, Y. Matsushita, *Macromolecules* **2005**, *38*, 10220.

[14] J. Masuda, A. Takano, Y. Nagata, A. Noro, Y. Matsushita, *Phys. Rev. Lett.* **2006**, *97*, 098301.

[15] J. Masuda, A. Takano, J. Suzuki, Y. Nagata, A. Noro, K. Hayashida, Y. Matsushita, *Macromolecules* **2007**, *40*, 4023–4027.

[16] P. J. Hoogerbrugge, J. M. V. A. Koelman, *Europhys. Lett.* **1992**, *19*, 155–160.

[17] R. D. Groot, P. B. Warren, *J. Chem. Phys.* **1997**, *107*, 4423–4435.

[18] C. I. Huang, C. M. Chen, *ChemPhysChem* **2007**, *8*, 2588–2594.

[19] R. D. Groot, T. J. Madden, *J. Chem. Phys.* **1998**, *108*, 8713–8724.